Charge Recombination in Conjugated Polymer/Fullerene Blended Films Studied by Transient Absorption Spectroscopy

Ana F. Nogueira, Ivan Montanari, Jenny Nelson, and James R. Durrant*

*Centre for Electronic Materials and Devices, Departments of Chemistry and Physics,
Imperial College, London SW7 2AY, United Kingdom*

Christoph Winder and Niyazi Serdar Sariciftci

*Linz Institute for Organic Solar Cells (LIOS), Physical Chemistry, Johannes Kepler University,
Altenbergerstrasse 69, A-4040 Linz, Austria*

Christoph Brabec

SIEMENS AG CT MM1-Innovative Electronics Paul-Gossenstrasse 100 35/409 D, 91052 Erlangen, Germany

Received: September 30, 2002; In Final Form: November 11, 2002

The recombination dynamics of long-lived photogenerated charge carriers are investigated by transient absorption spectroscopy (TAS) on micro- to millisecond time scales in a blend of poly[2-methoxy-5-(3′,7′-dimethyloctyloxy)-1-4-phenylene vinylene], (MDMO-PPV) and 1-(3-methoxycarbonyl)propyl-1-phenyl-(6,6)-C_{61} (PCBM) at room temperature. In this work we focus on the physical origins of these recombination dynamics. Studies are conducted as a function of blend composition (including consideration of pristine MDMO-PPV films), solvent, temperature, and the effect of white light bias. We conclude that following low-intensity excitation of the MDMO-PPV/PCBM blend, MDMO-PPV polarons are trapped in an inhomogeneous distribution of localized states ($\sim 10^{17}$ cm^{-3}) above the mobility edge for the polymer valence band. The recombination dynamics of these polarons with PCBM anions are limited by the thermally activated detrapping of these polarons, being rather insensitive to both PCBM anion dynamics and MDMO-PPV/PCBM phase segregation. Steady-state white light illumination results in the continuous occupancy of the tail of these localized states, causing an acceleration of the recombination dynamics. These observations are discussed in terms of their relevance to device function.

Introduction

The discovery of ultrafast, photoinduced charge transfer from a conjugated polymer to C_{60} (buckminsterfullerene)[1,2] has led to extensive academic and commercial interest in the development of solar cells and photodiodes employing these materials.[3,4] $\pi \rightarrow \pi^*$ photoexcitation of the conjugated polymer results in electron transfer to the fullerene molecule, leaving a positive delocalized charge (polaron) on the polymer. Early photovoltaic devices, fabricated from conjugated polymer/C_{60} bilayers, yielded low power conversion efficiencies, as the film thickness required for efficient light absorption by such polymers (>100 nm) is significantly greater than the exciton diffusion length ($\sim$10 nm). A breakthrough for these polymer solar cells was the introduction of the bulk heterojunction concept.[5,6] Mixing or blending a soluble methanofullerene directly into the conjugated polymer film leads to a three-dimensional heterojunction on the nanometer scale.[7] The blending of the electron and hole transporting materials ensures efficient charge separation, because excitons are photogenerated within the exciton diffusion length of fullerene electron acceptors. Initial devices fabricated using this concept exhibited efficiencies under AM 1.5 illumination of approximately 1%.[5] Morphology[8–10] and improved electrical contact interfaces have been shown to be

crucial parameters for optimizing device efficiency. Efficiencies of up to 3.3% have now been reported for devices produced by casting blends of poly[2-methoxy-5-(3′,7′-dimethyloctyloxy)-1-4-phenylene vinylene], (MDMO-PPV) and 1-(3-methoxycarbonyl)-propyl-1-phenyl-(6,6)C_{61} (PCBM) MDMO-PPV/PCBM in a 1:4 ratio (w/w) from chlorobenzene.[4,11,12]

The bulk heterojunction approach is attractive for achieving high charge separation efficiency. However, a limitation of the intimate blending achieved in such films is that electrons and holes transporting materials are not spatially well separated. Consequently, charge recombination losses can be expected to be a factor limiting device performance, but have received only limited attention to date. Of particular relevance, it has been found that optimum device performance is achieved with film thickness of $\sim$100 nm, significantly less than that required for efficient light absorption, indicative of significant recombination losses preventing efficient charge carrier collection in thicker films. Understanding the parameters influencing recombination dynamics in polymer/fullerene blends is therefore likely to be critical in optimizing device performance, and is the primary motivation for the studies reported here.

Charge separation in polymer/fullerene blends results in generation of negative charge on the fullerene and a positive hole in the HOMO level (valence band) of the polymer. Electron transport proceeds by electron hopping between adjacent fullerene molecules. The use of a high concentration of C_{60}

* Corresponding author. Fax: 44 (0)20 7594 5801. E-mail: j.durrant@ic.ac.uk.

molecules in the blend is essential to ensure continuous pathways for this electron transport.[4] The positive hole on the polymer is typically associated with significant local deformation of the polymer structure, and is therefore referred to as a polaron. The density of polaron states in conjugated polymers is typically inhomogeneous broadened by local variations in polymer structure. This conformational disorder has a strong influence upon polaron mobility, resulting in a tail of relatively localized polaron states extending above the valence band into the band gap of the material.[13]

Previous studies of recombination dynamics in polymer/fullerene blends have been rather limited, typically employing frequency domain techniques, often referred to as "photoinduced absorption" or PIA studies. As such studies are limited to frequencies <10 kHz, they have primarily been conducted at low temperatures in order to increase the lifetime of the photoinduced charge carriers. The lifetime of the charge separated state was estimated with such a technique to be of the order of milliseconds at 80 K.[2] In contrast to these frequency domain measurements, time domain transient absorption spectroscopy (TAS) employing pulsed laser excitation has typically focused on recombination dynamics in polymer/fullerene films on the picosecond and nanosecond time scales.[14-15]

We have recently reported a transient absorption study of the dynamics of charge recombination in a MDMO-PPV/PCBM blend film at room temperature.[16] In that study we reported two decay phases of photogenerated MDMO-PPV polarons with time scales of <20 ns and 300 ns–10 ms, both decay phases being attributed to recombination of polarons with PCBM anions. The amplitude of the fast decay component was observed to be strongly dependent upon the intensity of the excitation laser pulses, and exhibited negligible amplitude for excitation densities ≤ 1 μJ cm^{-2}. In contrast, the amplitude of the slow, 300 ns–10 ms decay phase was independent of excitation density in the range 1 to 80 μJ cm^{-2}, and was only reduced in amplitude for excitation densities <1 μJ cm^{-2}. In this paper, we focus on the physical origins of these recombination dynamics. Studies are conducted as a function of blend composition, including pristine MDMO-PPV films, solvent, temperature, and the effect of white light illumination. Our studies address particularly the origin of the slow decay phase. This phase is likely to be particularly relevant to photovoltaic device function as it dominates the decay dynamics at low laser intensities, conditions most comparable to steady-state solar irradiation.

Experimental Methods

The conjugated polymer used as electron donor in this work was poly[2-methoxy-5-(3′,7′-dimethyloctyloxy)-1-4-phenylene vinylene] (MDMO-PPV), whereas the electron acceptor was 1-(3-methoxycarbonyl)-propyl-1-phenyl-(6,6)C61 (PCBM). The enhanced solubility of PCBM compared to C_{60} allows a high fullerene/conjugated polymer ratio and enables the formation of donor/acceptor bulk heterojunctions. The active layer was spin-coated onto a glass substrate from solutions of MDMO-PPV and PCBM (ratios of 4:1 to 1:6 by weight) in chlorobenzene or toluene solutions, resulting in a film thickness of ~100 nm. Chlorobenzene solutions were routinely employed, unless otherwise stated. Pristine MDMO-PPV samples were prepared using the same procedure. Following fabrication, the films were maintained under a nitrogen or argon atmosphere and stored in the dark until used. UV/visible spectra recorded before and after transient absorption experiments did not indicate any sample degradation. Transient absorption data were collected with the

sample held in a glass cuvette under a nitrogen atmosphere. For experiments carried out at low temperatures, the samples were kept inside a temperature-controlled Oxford Instruments DN-V vacuum cryostat at sample temperatures between 80 and 300 K.

Micro- to millisecond transient absorption spectroscopy was carried out using a nitrogen laser pumped - dye laser as excitation source (repetition rate 4 Hz, pulse duration < 1 ns) and a tungsten lamp with a stabilized power supply as a probe light. The excitation wavelength was 500 nm, corresponding to the absorption maximum of MDMO-PPV (optical density of 0.2–2.5 depending upon blend composition). The transient absorption signal was typically collected at a probe wavelength of 940 nm, corresponding to the maximum of the absorption of the photoinduced transient signal, assigned to absorption of MDMO-PPV$^+$ polarons.[16] The probe wavelength was selected by two monochromators before and after the sample, which minimize the amount of probe light incident on the sample and the amount of scatter/emission reaching the photodetector, respectively. A high gain photodiode equipped with appropriate low and high pass filtering was employed as the detection unit. The instrument response was of the order of 300 ns. Data were collected on time scales from 10 μs to 10 ms, averaging typically 300–1000 laser shots on each time scale, yielding a sensitivity of 10^{-6} to 10^{-4} depending upon the time scale under study. Data are plotted as the change in sample optical density ΔOD, which is related to the change in sample transmission ΔT by ΔOD $\times$ ln 10 $= -\Delta T/T$. Experiments as a function of the excitation power employed neutral density filters to vary the laser intensity from 20 nJ to 80 μJ m^{-2} per pulse. Experiments with improved instrument response (~20 ns) were conducted as reported previously, employing an 830 nm laser diode as probe light source.[16] Experiments under continuous white light were performed by using the first monochromator in reflection mode, resulting in ~25 mW/cm^2 of white light incident upon the sample.

Results

Recombination Dynamics as a Function of Excitation Density. Figure 1a shows the room-temperature transient absorption kinetics observed for a MDMO-PPV/PCBM blend on the micro- to millisecond time scale using excitation densities ranging from 20 nJ to 80 μJ cm^{-2} per pulse (corresponding to 5×10^{10} to 2×10^{14} photons cm^{-2} per pulse). The samples were excited at 500 nm and the decay of the transient signal, corresponding to the decay of positive MDMO-PPV polarons, was measured at 940 nm.[16] The inset shows an extension of these studies to the nanosecond time scale, as reported in ref 16, showing the fast (<20 ns) decay phase observed at high laser intensities. It is apparent that for time delays greater than 300 ns, the transient signal is independent of laser intensities for excitation densities >2 μJ cm^{-2}, with the signal only exhibiting a dependence upon excitation intensity for densities <2 μJ cm^{-2}. This slow decay phase is approximately linear on log/log plots, as shown previously,[16] indicating the polaron density, p, follows a power law with time, t

$$p \propto t^{-\alpha}$$

From the gradient of the decays, we obtain a value of 0.4 $\pm$ 0.05 for the exponent, α, at room temperature.

Both the <20 ns and 300 ns–10 ms decay phases are assigned to recombination of photogenerated MDMO-PPV$^+$ polarons and PCBM anions.[16] We have previously suggested that the slow

Charge Recombination in Polymer/Fullerene Solar Cells

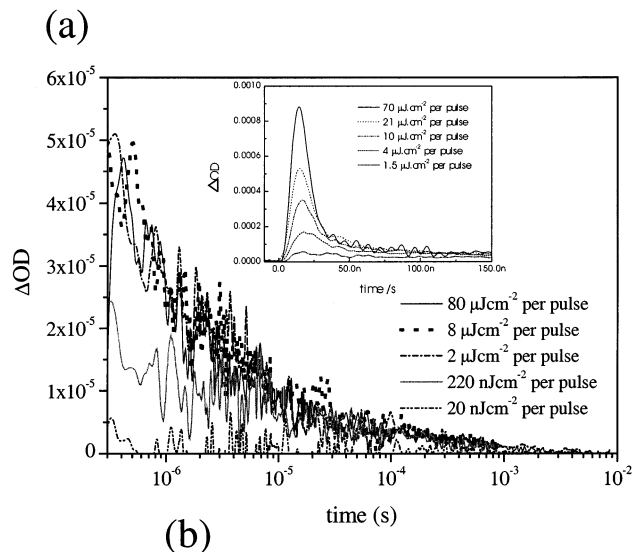*J. Phys. Chem. B, Vol. 107, No. 7, 2003* **1569**

Figure 1. (a) Transient absorption kinetics for 1:4 w/w MDMO-PPV/PCBM blend films on the microsecond-millisecond time scale as a function of excitation density. The excitation densities ranged between 20 nJ to 80 μJ cm^{-2} per pulse. The decay is assigned to charge recombination between PCBM anions and MDMO-PPV$^+$ polarons. Data were collected using a probe wavelength of 940 nm, corresponding to an absorption maximum of MDMO-PPV$^+$ polarons, at room temperature (296 K). It is apparent the transient signal is independent of excitation density in the range 2 to 80 μJ cm^{-2} per pulse. The inset shows analogous data collected on the nanosecond time scale from 1.5 to 70 μJ cm^{-2} per pulse as previously reported in ref 16. (b) Simple model for charge recombination in these blends at low and high excitation density showing a tail of localized states that extend above the effective mobility edge for the material's valence band.

phase (referred to hereafter as the ns-ms decay phase) is assigned to the dynamics of MDMO-PPV$^+$ trapped in a tail of localized states above the MDMO-PPV valence band, with the power law behavior resulting from the inhomogeneous energetics of these states. The saturation in the amplitude of this phase for excitation intensities >1 μJ cm^{-2} was attributed to the density of photogenerated MDMO-PPV$^+$ polarons exceeding the density of available localized states. As 1 μJ cm^{-2} corresponds to ~10^{12} absorbed photons cm^{-2} (optical density of 100 nm thick film being 0.3), this corresponds to a ~10^{17} cm^{-3} density of these localized states, assuming a unity quantum yield for charge separation.[12] The fast, <20 ns, phase is then assigned to mobile MDMO-PPV$^+$ polarons generated when the density of photogenerated polarons exceeds the density of localized states. These assignments are illustrated in Figure 1b. We present below a systematic study of the parameters influencing the slower ns-ms power law decay phase and the extent to which these observations are consistent with the simple model illustrated in Figure 1b.

Comparison with Pristine PPV Films. A key issue for consideration of the recombination data shown in Figure 1 is the extent to which the dynamics are controlled by polaron dynamics in the MDMO-PPV, electron hopping between PCBM molecules, or interfacial electron-transfer dynamics between
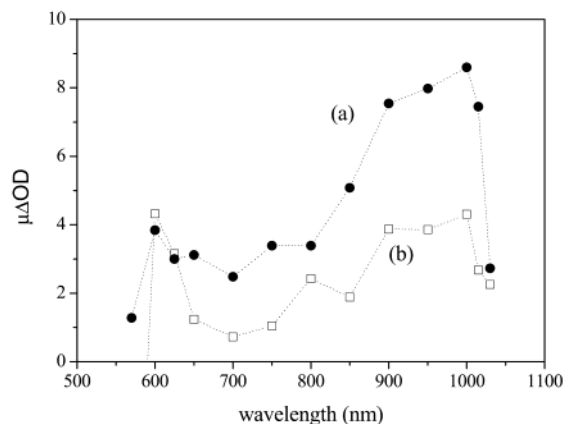

Figure 2. Transient absorption spectra obtained 125 μs after excitation at 500 nm of (a) 1:2 w/w MDMO-PPV/PCBM blend, and (b) pristine MDMO-PPV films ($T = 300$ K).
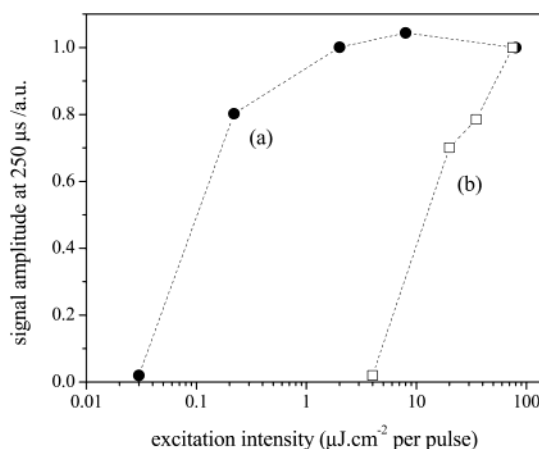

Figure 3. Relative amplitude of the transient absorption signal for the blend MDMO–PPV/PCBM (--●--) and for the pristine polymer (--□--) as a function of laser excitation density. Data shown employed a 940 nm detection wavelength, with data amplitude averaged between 100 and 400 μs. Other experimental conditions as for Figure 2.

these two phases. We consider first a comparison of polaron dynamics for a "standard" 1:4 w/w MDMO-PPV/PCBM blend with a pristine MDMO-PPV film.

Figures 2a and 2b show transient absorption spectra of films of the MDMO-PPV/PCBM blend and the pristine MDMO-PPV measured at 125 μs after pulsed excitation (2 μJ cm^{-2} per pulse) at 500 nm ($T = 300$ K). The transient spectra for these two films are remarkably similar. Both spectra show the maxima at 1.2 to 1.5 eV and at 1.8 to 2.2 eV, features previously assigned to absorption of MDMO-PPV positive polarons.[16–18] We therefore conclude that, as for the MDMO-PPV/PCBM blend, optical excitation of the pristine MDMO-PPV results in formation of long-lived MDMO-PPV$^+$ polarons generated by photoinduced charge separation within the film. Radical anion absorptions of PCBM are generally much weaker in intensity and are located around 1.1 eV, these can therefore not be observed in these studies.

Figure 3 addresses the quantum yield for the generation of long-lived MDMO-PPV$^+$ polarons in the MDMO-PPV/PCBM blend and pristine MDMO-PPV films. The figure shows the laser power dependence of the MDMO-PPV$^+$ polaron signal amplitude averaged from 100 to 400 μs. As is already apparent from Figure 1, the polaron signal amplitude for the blend is independent of laser intensity for excitation densities greater than 1 μJ cm^{-2}, attributed to saturation of the density of localized
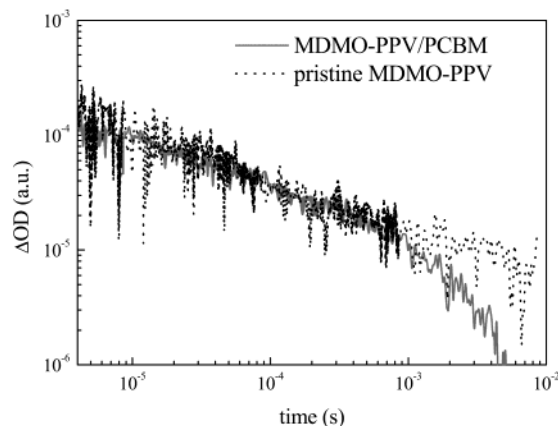
Figure 4. Comparison of the polaron decay kinetics of the MDMO-PPV/PCBM blend (1:6 by weight) and the MDMO-PPV pristine polymer on a log−log axes. Excitation intensities of 70 μJ cm^{-2} per pulse, other experimental details as Figure 2. The data have been normalized to the same amplitude at 10 μs to facilitate comparison It is apparent that the MDMO-PPV$^+$ decay dynamics are indistinguishable for the two films up to 1 ms; for time delays >1 ms an additional decay phase is observed for the blend, but not observed for the pristine film.

Figure 5. Transient absorption kinetics observed for 1:4 w/w MDMO-PPV/PCBM blends cast from chlorobenzene (*grey curve*) and toluene (*black dashes*) solutions. Experimental conditions as for Figure 4. It is apparent that the two samples exhibit indistinguishable MDMO-PPV$^+$ decay dynamics.

polaron states. For excitation densities lower than 1 μJ cm^{-2}, the amplitude is dependent upon laser intensity, corresponding to conditions where the density of photogenerated MDMO-PPV polarons no longer exceeds the density of localized states ($\sim$10^{17} cm^{-3}). In contrast to the blend signal, it is apparent that for the pristine MDMO-PPV film the amplitude of the transient signal is much more strongly dependent upon the excitation density, and does not saturate over the laser intensity range studied (up to 70 μJ cm^{-2}). At lower excitation densities, the polaron signal is much smaller for the pristine MDMO-PPV film than for the blend; for example at 4 μJ cm^{-2}, the signal for the pristine signal is negligible, while the blend signal remains saturated at its maximal value. It can be concluded that the yield of polaron formation is much lower for the pristine film than for the blend, consistent with previous observations that photoinduced electron transfer from the polymer to the fullerene improve the quantum efficiency for photogeneration of charge carriers in blended films.[19] At high laser powers, the long-lived polaron signals are of similar magnitude, consistent with saturation of the density of localized polarons states in the MDMO-PPV, with the excess polarons formed in the blend recombining on the nanosecond time scale (as discussed above). Comparison of the excitation density data shown in Figure 3 indicates that the quantum yield for polaron formation in the pristine film is at least 100-fold lower than that of the blend, consistent with the difference in luminescence yields of the two films, with the blend photo-luminescence being quenched by >100 relative to the pristine film.[1,2]

We turn now to a comparison of the decay dynamics of the long-lived MDMO-PPV polarons photogenerated in the blend and pristine films, as shown in Figure 4. The decay of the transient signals for the blend and for the pristine material are remarkably similar over the time range 400 ns−1 ms. For time delays >1 ms, the blend signal exhibits an additional decay phase not present for the pristine material. We note that the nature of charge recombination is different for the two films—in the blend the recombination is between localized MDMO-PPV$^+$ polarons and PCBM anions and for the pristine material it is between localized MDMO-PPV$^+$ polarons and negative polarons, reduced defects, or impurities. The observation of similar decay dynamics for both films indicates that the
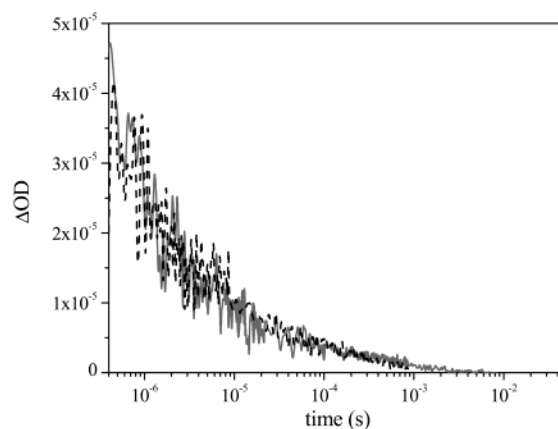
recombination dynamics between 400 ns and 1 ms are primarily controlled by the dynamics of the localized MDMO-PPV$^+$ polarons present in both films and are independent of nature of the acceptor molecules present. It can furthermore be concluded that phase segregation, thought to be present in the MDMO-PPV/PCBM blended film[20] but obviously absent in the pristine MDMO-PPV film, has negligible influence on the recombination dynamics on this time scale. The appearance of an additional decay phase in the blend material for time delays >1 ms suggests that this decay phase is associated with the dynamics of PCBM anions in the blend, as we will discuss in detail below.

Further studies were conducted as a function of blend composition with blend ratios ranging from 4:1 to 1:6 MDMO-PPV/PCBM by weight. As expected from the data shown in Figure 4, the presence of the additional >1 ms decay phase was dependent upon PCBM concentration in the film, with this phase only being clearly resolved for MDMO-PPV/PCBM blend ratios of 1:4 or more PCBM by weight.

Recombination Dynamics as a Function of Blend Deposition Conditions. Shaheen et al. have reported that the mechanical and electrical properties of the photoactive layer in polymer/fullerene solar cells is strongly influenced by the casting conditions.[20] They compared the morphologies and photovoltaic performances of blends cast from chlorobenzene and toluene solutions. Casting from chlorobenzene resulted in the preparation of devices with a 3-fold increase in the overall photovoltaic efficiency. This improvement was attributed to reduced phase segregation of the MDMO-PPV and PCBM components due to the higher solubility of PCBM in this solvent, as evidenced by AFM studies indicating a much smoother film surface for this solvent. Figure 5 compares decay dynamics for 1:4 w/w MDMO-PPV/PCBM blend films deposited from chlorobenzene and toluene solutions. Despite the inferred difference in the morphology of these blends, it is apparent that the charge recombination dynamics observed for the two films are indistinguishable. This observation provides further support for our conclusion above that the charge recombination dynamics are indeed controlled by MDMO-PPV$^+$ polarons dynamics in polymer bulk rather than by interfacial processes associated with phase segregation of the blend. We note this result contrasts with the observation that the mobility of the positive charge carriers in chlorobenzene cast films increases relative to that of the toluene cast films, as measured in field effect transistor geometry (Wim Geens et al., in press). It is not straightforward
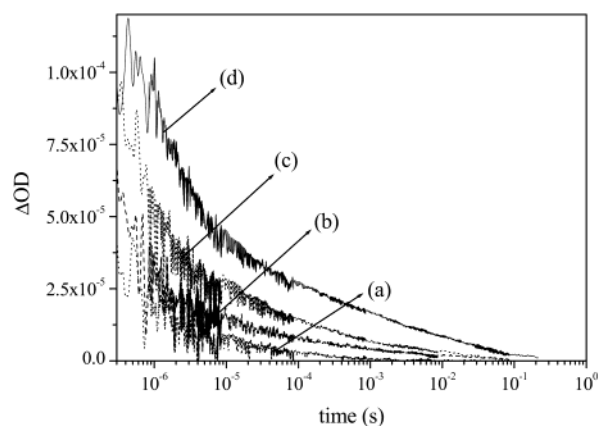
Charge Recombination in Polymer/Fullerene Solar Cells

J. Phys. Chem. B, Vol. 107, No. 7, 2003 **1571**

Figure 6. Transient absorption kinetics observed for a 1:4 w/w MDMO-PPV/PCBM blend as a function of sample temperature: (a) 300 K; (b) 220 K; (c) 150 K; (d) 80 K. Excitation intensity of 70 μJ m^{-2} per pulse, other experimental conditions as for Figure 1.

to correlate the mobility of carriers with the recombination dynamics of them, thus further studies are underway to clarify this effect.

Temperature Dependence of the Recombination Dynamics. We have assigned the kinetics of the ns-ms power law decay phase of transient signal to the recombination dynamics of localized MDMO-PPV$^+$ polarons. A key consideration for the nature of these localized states is whether the polarons recombine via thermal activation to states above the mobility edge followed by diffussion to anion sites, or via a temperature-independent tunneling process. To address this issue, we collected transient absorption data for film temperatures between 300 and 80 K.

Figure 6 shows the temperature dependence of the MDMO-PPV$^+$ decay for blends of MDMO-PPV/PCBM (1:2 w/w) at 300, 220, 150, and 80 K. Cooling the film from 300 to 220 K results in a significant retardation of the recombination dynamics. This retardation can be quantified by fitting the data to the power law decay given in eq 1, which indicates that lowering the temperature from 300 to 220 K results in a decrease in the value of α from 0.41 to 0.3. This retardation is strongly indicative of a thermally activated process. Further cooling below 220 K primarily results in an increase in signal amplitude. We note however that, following prolonged sample cooling to 80 K, this increase in amplitude was irreversible. This increase in amplitude therefore appears to originate, at least in part, from an irreversible change in the sample, most probably associated with a change in morphology and therefore in the density of localized MDMO-PPV$^+$ states.

Influence of Continuous White Light Illumination. Photovoltaic devices operate under continuous white light illumination. To investigate the influence of such continuous illumination upon the charge recombination dynamics, transient absorption data similar to those reported above were collected in the presence of ~25 mW cm^{-2} of continuous background white light illumination. The transient absorption signals in the presence and absence of this white light were obtained at 220 and 300 K as shown in Figure 7. It can be seen that at both temperatures the white light does not influence the initial amplitudes of the signals, but does result in faster decay dynamics at longer times, with in particular the slow tail of the recombination dynamics being lost at both temperatures.

Discussion

Optical excitation of the polymer/fullerene blends studied in this paper results in efficient charge separation, yielding
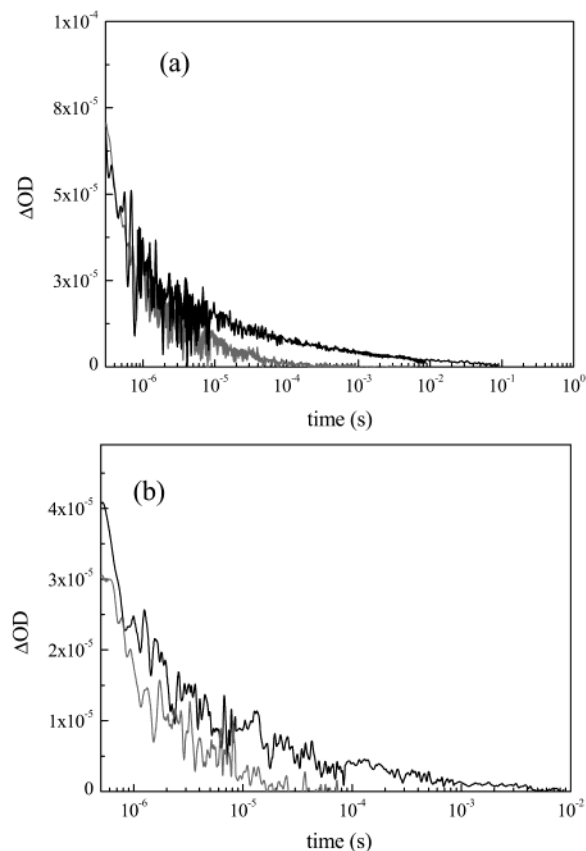

Figure 7. Comparison between transient absorption kinetics observed exciting a 1:2 w/w MDMO-PPV/PCBM blend cast from chlorobenzene in the dark (black curve) and under 25 mW cm^{-2} continuous white light illumination (gray curve) at different sample temperatures: (a) 220 K; (b) 300 K. Other experimental conditions as Figure 6.

MDMO-PPV positive polarons and PCBM anions. Efficient current generation by this blend requires these charge carriers to be collected by the device electrodes. Recombination of these charge carriers competes with this charge collection process. Several previous reports have studied such charge recombination dynamics on the nanosecond to picosecond time scales.[14−15,21−22] These fast recombination dynamics have been assigned to geminate recombination of charge carriers. However, as we have shown previously,[16] these fast recombination dynamics are only observed at high excitation intensities; employing low excitation densities more comparable to solar illumination, the recombination dynamics of such films in the absence of external electrodes occurs primarily on micro-millisecond time scales. These slower time scale recombination dynamics are attributed to trapped charge species, which we show here to be MDMO-PPV polarons trapped in a tail of localized states extending above the effective mobility edge for the material's valence band. In a functioning device, thermal relaxation of photogenerated MDMO-PPV polarons into these localized states is likely to compete with charge carrier collection by the electrodes, and may be a key factor influencing device performance.

In this paper, we address the parameters controlling the ns-ms phase of recombination dynamics observed for the MDMO-PPV/PCBM blend films (i.e., the dynamics between ~300 ns and 10 ms). Several key conclusions can be drawn:

1. *The ns-ms recombination dynamics are primarily controlled by the dynamics of MDMO-PPV$^+$ polarons in the bulk of the MDMO-PPV matrix.* The observation of similar recombination dynamics for both MDMO-PPV/PCBM blend and pristine MDMO-PPV films indicates that the recombination

dynamics are limited by dynamics of the localized MDMO-PPV^+ polarons rather than by the percolation of electrons through PCBM molecules or interfacial dynamics resulting from polymer/fullerene phase segregation.

2. These recombination dynamics are thermally activated. The recombination dynamics exhibit strong retardation when the temperature is reduced from 300 to 220 K, indicative of a thermally driven process controlling the recombination dynamics of the localized MDMO-PPV^+ polarons. We note that this observation suggests that zero temperature models of tunneling between spatial distributed localized states cannot be directly extended to room temperature. Such models have previously been employed to describe recombination dynamics in MDMO-PPV/PCBM blends at low temperatures (40 K).[23]

3. These recombination dynamics exhibit a power law decay. This power law decay, which has been reported previously in studies of analogous films at low temperatures,[22] is indicative of an inhomogeneous distribution of recombination/transport dynamics. In combination with (2) above, it is indicative of an energetic distribution of localized MDMO-PPV^+ polarons states lying above the polymer "valence band" mobility edge. In particular, a power law decay is consistent with thermal activation out of an *exponential* distribution of localized states, as we address in detail elsewhere.[24,26]

4. High PCBM concentrations in the blend (blend ratios greater than or equal to 1:4) result in an additional >1 ms MDMO-PPV^+ recombination phase. Following (2) and (3) above, the most deeply trapped MDMO-PPV^+ polarons recombine on the longest time scales. The decay dynamics of these deeply trapped polarons are found to be dependent on fullerene composition, suggesting that at such long times direct electron tunneling from PCBM anions to these trapped polarons may become important at high fullerene compositions. The initial ΔOD amplitude of this fullerene-dependent decay phase is ~1.5 × 10^{-5}, approximately 30 times less than the initial amplitude of the ns-ms power law decay phase, from which we estimate the density of these deeply trapped MDMO-PPV polaron states to be 3 × 10^{15} cm^{-3}.

5. Background illumination results in loss of the slowest tail of the recombination dynamics. Following from (3) above, background illumination results in continuous occupancy of the lowest energy localized MDMO-PPV^+ polaron states (i.e., those states furthest above the MDMO-PPV "valence band" mobility edge). Additional polarons generated by the laser excitation occupy shallower localized states, and are therefore relatively mobile, resulting in faster recombination dynamics. Since the lowest states are continuously occupied, the slow tail of the recombination dynamics, corresponding to de-trapping from the lowest-energy localized states, is not observed. The decay kinetics are dependent upon white light illumination for ΔOD signal magnitudes ≤3 × 10^{-5}, approximately 10 times less than the initial amplitude of the ns-ms power law decay phase. This indicates that our illumination conditions (~$^1/_4$ sun) result in a steady-state occupancy of approximately 10% of the localized MDMO-PPV polaron states, (i.e., ~10^{16} cm^3), and therefore concomitantly an equal density of PCBM anions.

Figure 8 illustrates the key features of the MDMO-PPV "valence band" density of states that can be inferred from the studies reported here. At low excitation densities, positive polarons relax on ultrafast time scales into the tail of relatively localized states extending above the mobility edge (Figure 8a). The total density of states in this tail is estimated to be 10^{17} cm^{-3}. At high excitation densities (>10^{17} photogenerated charge carriers per cm^3), this tail becomes fully occupied (Figure 8b).
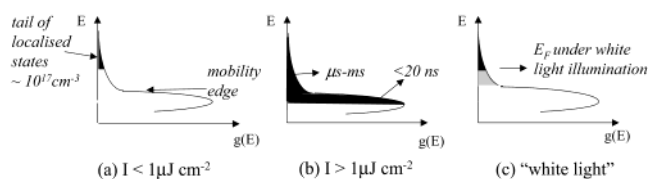

Figure 8. Simple model illustrating the influence of laser intensity (I) and white light illumination on the MDMO-PPV^+ polaron decay dynamics. The solid lines indicate the polaron density of states inferred from our studies, with a tail of 10^{17} cm^{-3} localized states extending above the main polymer valence band into the band gap. (a) Low laser excitation intensities results in only partial filling of the density of localized states, giving rise to power law recombination dynamics on the 300 ns-ms time scales. (b) At high laser intensities excess polarons occupy the non-localized states above the mobility edge of the valence band, giving rise to a fast (>20 ns) decay dynamics. (c) Continuous white light illumination results in occupancy of lowest energy localized states, resulting in laser-induced polarons occupying higher energy and therefore more mobile polarons, and thereby an acceleration of the recombination dynamics.

These conditions therefore result in the generation of relatively mobile polarons, at higher energy than the effective mobility edge for the material, which undergo rapid (<20 ns) recombination with photogenerated PCBM anions. Continuous illumination at ~$^1/_4$ solar irradiation results in the steady-state occupancy of ~10^{16} cm^{-3}, corresponding to only $^1/_{10}$th occupancy of the tail states (Figure 8c).

The shape of the MDMO-PPV polaron density of states illustrated in Figure 8 deviates significantly from that typically used in consideration of polaron charge transport in such materials. This density of states has been most widely considered to be Gaussian in shape, with typical widths of 100 meV.[25] The tail of states extending above the main valence band indicated by the present work has significant implications for the kinetics of charge transport in these devices. We will present elsewhere a detailed quantitative analysis of the charge recombination dynamics reported here, and their relevance to charge transport and collection in these materials.[26]

We have concluded above that the recombination dynamics of the long-lived charge carriers in MDMO-PPV/PCBM are limited by the detrapping dynamics of localized MDMO-PPV^+ polarons. This conclusion applies independent of PCBM anion concentration (except for the low amplitude >1 ms decay phase observed at high PCBM blend concentrations). We note that our studies do not address electron mobility in the PCBM. Localized MDMO-PPV^+ polarons spatially located away from PCBM moieties will be unable to recombine by direct electron tunneling, independent of the mobility of electrons in the PCBM. Such spatially localized polarons may only recombine by thermally activated detrapping, allowing polaron motion to the proximity of fullerene anion species. In this picture, the >1 ms phase we observe for high fullerene compositions may result from deeply trapped polarons where the rate of direct electron tunneling from fullerene anions exceeds the rate of thermally activated detrapping of the polaron.

The results reported here were collected for MDMO-PPV/PCBM films spin coated onto glass substrates in the absence of charge collecting electrodes. In a complete photovoltaic device polaron relaxation, and the subsequent recombination dynamics of the localized polarons as reported here, will be in competition with carrier collection by the electrodes and transfer to the external electrical circuit. Experiments to address the kinetic competition between these process are underway, and will be reported in detail elsewhere.

Charge Recombination in Polymer/Fullerene Solar Cells

J. Phys. Chem. B, Vol. 107, No. 7, 2003 **1573**

References and Notes

(1) Sariciftci, N. S.; Smilowitz, L.; Heeger, A. J.; Wudl, F. *Science* **1992**, *258*, 1474.

(2) Smilowitz, L.; Sariciftci, N. S.; Wu, R.; Gettinger, C.; Heeger, A. J.; Wudl, F. *Phys. Rev. B* **1993**, *47*, 13835.

(3) Sariciftci, N. S.; Braun, D.; Zhang, C.; Srdanov, V. I.; Heeger, A. J.; Stucky, G.; Wudl, F. *Appl. Phys. Lett.* **1993**, *62*, 585.

(4) Brabec, C. J.; Sariciftci, N. S.; Hummelen, J. C. *Adv. Funct. Mater.* **2001**, *11*, 15.

(5) Yu, G.; Gao, J.; Hummelen, J. C.; Wudl, F.; Heeger, A. J. *Science* **1995**, *270*, 1789.

(6) Yu, G.; Heeger, A. J. *J. Appl. Phys.* **1995**, *78*, 4510.

(7) Hummelen, J. C.; Knight, B. W.; Lepeq, F.; Wudl, F. *J. Org. Chem.* **1995**, *60*, 532.

(8) Yang, C. Y.; Heeger, A. *J. Synth. Met.* **1996**, *83*, 85.

(9) Chen, L.; Godovsky, D.; Inganäs, O.; Hummelen, J. C.; Janssen, R. A. J.; Svensson, M.; Andersson, M. R. *Adv. Mater.* **2000**, *18*, 1367.

(10) Brabec, C. J.; Sariciftci, N. S.; Hummelen, J. C. *Adv. Funct. Mater.* **2001**, *11*, 15.

(11) Brabec, C. J.; Shaheen, C.; Winder, C.; Sariciftci, N. S.; Denk, P. *Appl. Phys. Lett.* **2002**, *80*, 1288 .

(12) Brabec, C. J.; Shaheen, C.; Winder, C.; Sariciftci, N. S.; Denk, P. *Appl. Phys. Lett.* **2002**, *80*, 1288.

(13) Mott, S. N. *Conduction in Non-Crystalline Materials*; Clarendon Press: Oxford, 1987; 18.

(14) Kraabel, B.; Lee, C. H.; McBranch, D.; Moses, D.; Sariciftci, N. S.; Heeger, A. J. *Chem. Phys. Lett.* **1993**, *213*, 389.

(15) Mizrahi, U.; Shtrichman, I.; Gerhoni, D.; Ehrenfreund, E.; Vardeny, Z. V. *Synth. Met.* **1999**, *102*, 1182.

(16) Montanari, I.; Nogueira, A. F.; Nelson, J.; Durrant J.; Loi, M-A.; Winder., C.; Sariciftci, N. S.; Brabec, C. J. *Appl. Phys. Lett.* **2002**, *81,* 3001.

(17) Brabec, C. J.; Dyakonov, V.; Sariciftci, N. S.; Graupner, W.; Leising, G.; Hummelen, J. C. *J. Chem. Phys*. **1998**, *109,* 1185.

(18) Brabec, C. J.; Cravino, A.; Zera, G.; Sariciftci, N. S.; Kiebooms, R.; Vanderzande, D.; Hummelen, J. C. *J. Chem. Phys*. *B* **2001**, *105,* 1528.

(19) Lee, C. H.; Yu, G.; Moses, D.; Padbaz, K.; Zang, C.; Sariciftci, N. S.; Heeger, A. J.; Wudl, F. *Phys. Rev. B* **1993**, *48*, 15425.

(20) Shaheen, S. E.; Brabec, C. J.; Sariciftci, N. S.; Padinger, F.; Fromherz, T.; Hummelen, J. C. *Appl. Phys. Lett.* **2001**, *78*, 841.

(21) Kraabel, B.; Hummelen, J. C.; Vacar, D.; Moses, D.; Sariciftci, N. S.; Heeger, A. J.; Wudl, F. *J. Chem. Phys*. **1996**, *104*, 4267.

(22) Meskers, S. C. J.; van Hal, P. A.; Spiering, A. J. H.; Hummelen, J. C.; van der Meer, A. F. G.; Janssen, R. A. J. *Phys. Rev. B* **2000**, *61*, 9917.

(23) Shultz, N. A.; Scharber, M. C.; Brabec, C. J.; Sariciftci, N. S. *Phys. Rev. B* **2001**, *64*, 245210.

(24) Nelson, J. *Phys. Rev. B* **1999**, *59*, 15374.

(25) Bässler, H. *Phys. Status Solidi B* **1993**, *175*, 15.

(26) Nelson, J. *Phys. Rev. B*, in press.